JOURNAL OF PROPULSION AND POWER
Vol. 20, No. 5, September–October 2004

Technical Notes

TECHNICAL NOTES are short manuscripts describing new developments or important results of a preliminary nature. These Notes cannot exceed 6 manuscript pages and 3 figures; a page of text may be substituted for a figure and vice versa. After informal review by the editors, they may be published within a few months of the date of receipt. Style requirements are the same as for regular contributions (see inside back cover).

Performance Evaluation Method for Ideal Airbreathing Pulse Detonation Engines

Daniel E. Paxson*
NASA John H. Glenn Research Center at Lewis Field, Cleveland, Ohio 44135

Introduction

PULSE detonation engines (PDEs) are receiving much attention as a potential means for propulsion or as part of a propulsion system for future aerospace vehicles. One reason for this seems to be the promise of high efficiency as a result of the observation that the basic PDE cycle is thermodynamically similar to one that utilizes constant volume combustion.[1,2] However, the analytical work on which this thermodynamic similarity is based is necessarily simplified. As a result, it is often somewhat optimistic. More importantly, the analytical work tends to consider the PDE primarily as a stand-alone device, whereas many potential applications are envisioned in which it is a component in a propulsion system. Analysis of such systems requires a performance description of the PDE that can be combined with the additional components in a straightforward manner. Even in stand-alone applications, the PDE consists not just of a tube or tube bank. It is necessarily coupled to a nozzle (and an inlet), which is thermally limited.

The present work introduces a method for describing the performance of a PDE cycle that can be readily applied to different propulsion systems. The method utilizes data from an experimentally validated, one-dimensional, time-accurate, reactive, computational-fluid-dynamics (CFD) Euler solver[3–5] to provide results that are idealized because of the assumptions of the code, but realistic in that they capture the complex gas dynamics of the cycle.[6] Furthermore, the analysis allows straightforward examination of many cycle modifications that can affect performance such as partial fueling. Additionally, it accounts for the critical fact that not all particles passing through a PDE necessarily go through the same thermodynamic cycle. In this work, a performance map is obtained from integrated inlet and exhaust flux quantities computed by the code. These are then mass- or time-averaged to provide steady-state results. It will be shown that the PDE performance can be represented as a total pressure ratio that is a unique function of the total enthalpy ratio and a nondimensional heat addition parameter.

In the following sections, the method will be described, and the utility of the resulting performance map will be demonstrated through the presentation of several simplified PDE system studies. The performance map description will be preceded by a listing of the assumptions and simplifications and a description of the particular PDE cycle under consideration. The Euler code, with which performance data are generated, has been described in detail elsewhere in the literature.[3–7] Validation efforts including calculation of detonation speeds, postdetonative properties, grid independence, and comparison with experimental results can be found in Refs. 3–7.

Received 21 October 2002; accepted for publication 25 May 2004.

*Aerospace Engineer, 21000 Brookpark Road. Senior Member AIAA.

Assumptions and Simplifications

The assumptions and simplifications used in the code and analysis are listed here:

1) The PDE flow is one-dimensional, inviscid, and adiabatic.
2) The PDE flow contains a combination of only reactant or product.
3) Both reactant and product are calorically perfect gases with the same properties.
4) All reactant (air/fuel combination) entering the PDE is at the prescribed mixture ratio.
5) Valves on the PDE open and close instantaneously with no losses.
6) Detonation occurs nearly instantaneously once reaction commences regardless of the mixture composition.
7) The exhaust static pressure is identical to the inlet total pressure. This implies a static operating environment in the vicinity of the device (e.g., in a duct behind an inlet diffuser and preceding a nozzle). For portions of the cycle in which the exhaust flow is sonic, exit pressure is appropriately extracted from the interior of the computing domain.[7]

Cycle Description

The cycles computed in this study share some common features. Each represents a self-aspirated PDE with a single valve at the inlet and constant cross-section tubes. The code has been run until the developed wave cycle repeats itself indefinitely, and the integrated flux of mass into the device over one cycle matches the integrated flux of mass out. Each cycle completely empties and fills the tube once per cycle with either a fuel/air mixture or pure air. Each cycle accomplishes the filling and emptying process in the least amount of time possible. Thus, the inlet opens precisely when the internal pressure in the tube drops below the inlet total pressure and closes precisely when the volume required to fill the tube has entered. Detonation is initiated immediately after the inlet is closed by rapidly adding heat to the first numerical cell (via a source term), or by imposing a very brief (i.e., negligible mass and momentum flux) high-pressure, high-temperature boundary condition at the inlet. Either method yields similar results.

Performance Map Description

Consider the ideal PDE cycle just described with static boundary conditions. The mass-averaged total enthalpy of the exhaust flow can be written as

$$\bar{H}_e = \frac{\int_0^{t_{\mathrm{cycle}}} (H\rho u)\,\mathrm{d}t}{\int_0^{t_{\mathrm{cycle}}} (\rho u)\,\mathrm{d}t} \tag{1}$$

where $H = h + u^2/2$ is the total enthalpy, and t_{cycle} is the time period of one cycle. The inlet total enthalpy is assumed known. Unless explicitly stated, all quantities in this work are dimensionless. The time t is the physical time normalized by the characteristic wave transit time L/a^*, where a^* is the speed of sound at a chosen reference state and L is the tube length. The pressure p and density

ρ are normalized by their respective reference values, and the axial velocity u is normalized by a^*.

Integration of the mass, energy, and species equations in the tube over one cycle, along with the stipulation that the cycle is a limit cycle, will show that the ratio of the mass-averaged total exhaust enthalpy to the inlet total enthalpy, HR, can be written as

$$\bar{H}_e/\bar{H}_i = 1 + q_0(\gamma - 1)(1 - \bar{\dot{m}}_{\text{air}}/\bar{\dot{m}}_i) \tag{2}$$

where the ratio $\bar{\dot{m}}_{\text{air}}/\bar{\dot{m}}_i$ hereafter called the purge fraction is defined as

$$\bar{\dot{m}}_{\text{air}}/\bar{\dot{m}}_i = \frac{\int_0^{t_{\text{cycle}}}(\rho_{\text{air}}u_{\text{air}})\,\mathrm{d}t}{\int_0^{t_{\text{cycle}}}(\rho_i u_i)\,\mathrm{d}t} \tag{3}$$

Here, the subscript air refers to the portion of the inlet flow which is pure air, and the subscript i refers to the total inlet flow of both pure air and reactant (air/fuel mixture).

The quantity q_0 is defined as

$$q_0 = \frac{\Delta h_f}{(1 + a/f)_\gamma R_g T^*} \tag{4}$$

where γ is the ratio of specific heats, a/f the air-to-fuel ratio, Δh_f the heat of reaction of fuel, R_g the gas constant, and T^* the reference temperature. Thus, the total enthalpy ratio HR is a function of the fuel property, the ambient enthalpy, the mixture stoichiometric ratio, and the purge fraction.

The time-averaged static specific thrust of a given cycle can be calculated as[8]

$$T_{\text{sp}}\left(g_c/a^*\right) = (MF_e - p_{0i}t_{\text{cycle}}/\gamma)/\bar{\dot{m}}_i \tag{5}$$

where p_{0i} refers to the inlet total pressure and g_c is the Newton constant. The subscript e refers to the exit plane. The momentum term MF_e is defined as

$$MF_e = \int^{t_{\text{cycle}}}\left(\frac{p_e}{\gamma} + \rho_e u_e^2\right)\mathrm{d}t \tag{6}$$

The equivalent exhaust total pressure $\bar{p}_{0e}$ for the device is then defined as the total pressure from which a gas at the mass-averaged total enthalpy defined by Eq. (2) must be ideally expanded (i.e., through a nozzle) to the ambient pressure p_{0i} in order to yield the same specific thrust as that calculated from Eq. (5). To obtain $\bar{p}_{0e}$, an equivalent exit velocity $\bar{u}_e$ can be defined from Eq. (5) because

$$\bar{u}_e = T_{\text{sp}}\left(g_c/a^*\right) = (MF_e - p_{0i}t_{\text{cycle}}/\gamma)/\bar{\dot{m}}_i \tag{7}$$

The equivalent total pressure can then be found from the average total enthalpy of Eq. (1) using

$$\bar{p}_{0e} = p_{0i}\Big/\left(1 - \bar{u}_e^2\big/2\bar{H}_e\right)^{\gamma/(\gamma-1)} \tag{8}$$

With the simplifications and cycle stipulations described earlier, it can be seen from Eqs. (2) and (8) that the pressure ratio $\text{PR} = \bar{p}_{0e}/p_{0i}$ is uniquely defined by q_0 and the purge fraction. Figure 1 shows PR as a function of the enthalpy ratio for various mixture heats of reaction q_0. For each q_0, the enthalpy ratio was varied by changing the purge fraction. The largest value of enthalpy ratio for each curve represents the minimum allowable purge fraction of approximately 2%. Attempts to further reduce the purge fraction resulted in autoignition. The minimum enthalpy ratio represents an arbitrarily chosen maximum purge fraction of approximately 70%, except for the $q_0 = 7.8$ case where it was 50%. The ratio of specific heats for all calculations was $\gamma = 1.3$. The number of numerical cells used in all of the calculations to be shown was 200. It can be seen that for a specified temperature ratio, the higher the purge fraction, the better the performance.

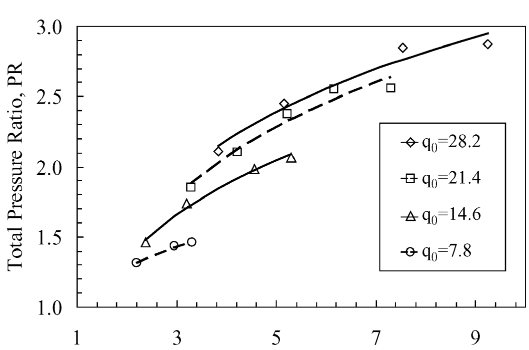

Fig. 1 Average total pressure ratio as a function of total enthalpy ratio for several families of q_0.

Application

With the performance of the PDE in the form just described, analysis for a variety of applications is readily possible.

Simple Brayton-Cycle Comparison

The PDE cycle is often compared with the Brayton cycle, the latter being representative of conventional turbomachinery-based propulsion systems. When this comparison is made however, it is not always clear that the parameters held in common are meaningful. What, for example, is the equivalent state in a PDE cycle to the compressor discharge of a Brayton cycle? Figure 2 shows a comparison in terms that are unambiguous. The performance of each cycle is plotted as PR vs HR as in Fig. 1. For the PDE cycle, all of the computed data have been plotted along with a simple curve fit defined by

$$\text{PR} = \text{HR}^{[0.120\gamma/(\gamma-1)]} \tag{9}$$

This curve fit further simplifies the computed results by assuming that, for the most part, varying HR by either q_0 or purge fraction yields equivalent results. It is noted that Eq. (9) has no theoretical basis and has not been tested for other values of γ. It is intended purely as a convenient fit for the data at hand.

Also shown in Fig. 2 are the results from a simple, nonideal Brayton cycle calculation[9] with compressor and turbine adiabatic efficiencies set to 0.85 and 0.90, respectively. The Brayton cycle results are shown for families of T_4/T_1, which is the ratio of turbine inlet temperature to compressor inlet temperature. For each family, the compressor pressure ratio π_c has been varied from 4 to 30, which is representative of modern turbomachinery. Because cycle efficiency increases monotonically with PR, it is clear that, within the temperature range of conventional turbomachinery shown, the Brayton cycle is more efficient than the PDE cycle as computed in the present work. To achieve higher temperature ratios, a Brayton cycle with an afterburning process would be required. This is discussed in the next example.

PDE with Inlet and Nozzle

As a second example of the application of the performance methodology, consider a PDE (or series of PDE tubes) with only an ideal inlet and nozzle fore and aft. Such a configuration can be envisioned for a high-speed, Mach 0-5 aircraft. Standard thermodynamic analysis[9] and Fig. 1, or more easily, Eq. (9), can be used

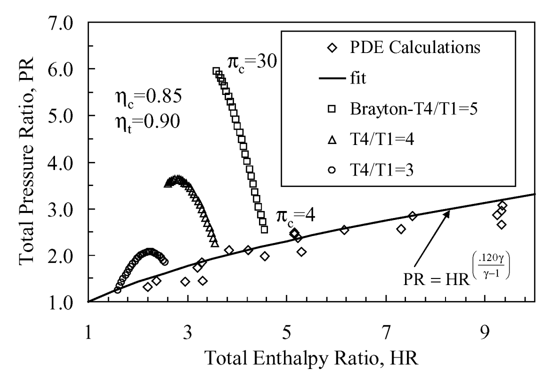

Fig. 2 Comparison of average total pressure ratio as a function of total enthalpy ratio for PDE and Brayton cycles. The ratio of specific heats, $\gamma = 1.3$.

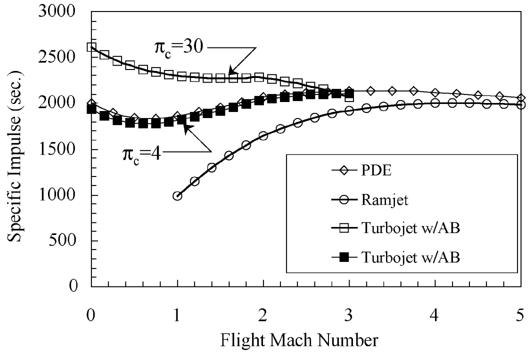

Fig. 3 Specific impulse as a function of Mach number for PDE, ramjet, and turbojet with afterburner. For all systems $\gamma = 1.3$, inlet and nozzle are ideal, and the nozzle inlet temperature is 4200 R (2300 K). For the turbojet, adiabatic compressor and turbine efficiencies are 0.85 and 0.90, respectively. The turbine inlet temperature is 3000 R (1670 K). The fuel heating value is 19,000 BTU/lb$_m$ (44,000 kJ/kg).

to calculate the specific thrust and specific impulse over the Mach-number regime. The specific impulse results are shown in Fig. 3. A Mach-number dependent static inlet temperature profile was used for these calculations in order to account for altitude effects.[7] The nozzle inlet total temperature was chosen to be 4200 R (2300 K). The ratio of specific heats was 1.3. The fuel heating value was 19,000 BTU/lbm (44,000 kJ/kg), typical for many hydrocarbon fuels.

Also shown in the Fig. 3 are the performance results for a ramjet and for afterburning turbojets with compressor pressure ratios of 30 and 4. For the turbojet calculations the compressor and turbine adiabatic efficiencies were again 0.85 and 0.90, respectively. The combustor and afterburner were assumed loss free (i.e., constant total pressure). The turbine inlet temperature was 3000 R (1670 K). It can be seen that the ideal PDE performance is fairly consistent over the Mach-number regime and that it is comparable with a non-ideal, afterburning turbojet having a compressor pressure ratio of 4.0. For turbojets of a more realistic pressure ratio, the PDE shows significantly less specific impulse and (not shown) specific thrust. Compared with the ramjet, the performance advantages of a PDE are clear at Mach numbers below 3.0. Beyond this, there does not appear to be significant benefit. These PDE performance results are smaller than what is typically listed in the literature[1,2,10]; however, because they represent computed results from a validated code, it can be argued that they are more representative of an idealization in the sense of being as good as can be expected.

Other PDE applications can be examined in a straightforward manner using the map of Fig. 1. Examples would include gas-turbine topping cycles, afterburners (bypass duct or full flow), even ejector-based cycles (if some assumptions are made regarding the work transfer process).

Of the applications that have been examined, the process has been made easier through the use of Eq. (9); however, it should be kept in mind that for a given application, not all values of q_0 (and therefore enthalpy ratio) are possible. Also, the results shown represent a particular gasdynamic cycle. Other cycles, such as PDE cycles with valved exhaust (or low-loss, variable backpressure systems), or those employing shaped tubes can lead to different and possibly superior performance to that presented.[11,12]

Conclusions

It has been demonstrated in this work that idealized airbreathing PDE performance can be mapped onto a single plot of total pressure ratio vs total enthalpy ratio. It has further been shown that this format is useful in system studies because the PDE can be viewed as simply another component with straightforward input and output. The idealized PDE performance data were obtained from a one-dimensional CFD code, and it has been shown that this is a more realistic approach than purely analytical methods. The performance shown is generally below that which has been previously reported for so-called idealized PDE performance but is still idealistic in that the losses captured are only those endemic to the cycle. A similar map that incorporates losses such as those caused by heat transfer, viscous effects, and valving could easily be generated.

References

[1] Heiser, W. H., and Pratt, D. T., "Thermodynamic Cycle Analysis of Pulse Detonation Engines," *Journal of Propulsion and Power*, Vol. 18, No. 1, 2002, pp. 68–76.

[2] Kentfield, J. A. C., "Fundamentals of Idealized Air-Breathing Pulse-Detonation Engines," *Journal of Propulsion and Power*, Vol. 18, No. 1, 2002, pp. 77–83.

[3] Nalim, R. M., and Paxson, D. E., "A Numerical Investigation of Premixed Combustion in Wave Rotors," *Journal of Engineering for Gas Turbines and Power*, Vol. 119, No. 3, 1997, pp. 668–675; also ASME Paper 96-GT-116, June 1996.

[4] Paxson, D. E., "Numerical Simulation of Dynamic Wave Rotor Performance," *Journal of Propulsion and Power*, Vol. 12, No. 5, 1996, pp. 949–957.

[5] Paxson, D. E., "A General Numerical Model for Wave Rotor Analysis," NASA TM 105740, July 1992.

[6] Wilson, J., and Paxson, D. E., "On the Exit Boundary Condition for One-Dimensional Calculations of Pulsed Detonation Engine Performance," NASA TM 2002-211299, July 2001.

[7] Paxson, D. E., "A Performance Map for Ideal Air Breathing Pulse Detonation Engines" AIAA Paper 2001-3465, July 2001.

[8] Foa, J. V., *Elements of Flight Propulsion*, Wiley, New York, 1960, pp. 266–273.

[9] Oates, G. C., *Aerothermodynamics of Gas Turbine and Rocket Propulsion*, AIAA, Reston, VA, 1997, pp. 231–275.

[10] Kailasanath, K., "A Review of PDE Research-Performance Estimates," AIAA Paper 2001-0474, Jan. 2001.

[11] Cambier, J. L., and Tegner, J. K., "Strategies for Pulsed Detonation Engine Performance Optimization," *Journal of Propulsion and Power*, Vol. 14, No. 4, 1998, pp. 489–498.

[12] Paxson, D. E., "Optimal Area Profiles for Ideal Single Nozzle Air-Breathing Pulse Detonation Engines," AIAA Paper 2003-4512, July 2003.

Impulse Correlation for Partially Filled Detonation Tubes

M. Cooper* and J. E. Shepherd†
California Institute of Technology, Pasadena, California 91125
and
F. Schauer‡
Air Force Research Laboratory, Wright–Patterson Air Force Base, Ohio 45433

Introduction

THE effect of nozzles on the impulse obtained from a detonation tube of circular cross section has been the focus of many experimental and numerical studies. In these cases, the simplified detonation tube is closed at one end (forming the thrust surface) and open at the other end, enabling the attachment of an extension. A flowfield analysis of a detonation tube with an extension requires considering unsteady wave interactions making analytical

Received 8 September 2003; revision received 5 February 2004; accepted for publication 15 March 2004.

*Graduate Student, Mechanical Engineering, Graduate Aeronautical Laboratories, MC 205-45.

†Professor, Aeronautics, Graduate Aeronautical Laboratories, MC 205-45. Member AIAA.

‡Propulsion Directorate.